A radiopaque calcium phosphate bone cement with long-lasting antibacterial effect: From paste to injectable formulation

A RADIOPAQUE CALCIUM PHOSPHATE BONE CEMENT WITH LONG-LASTING ANTIBACTERIAL EFFECT: FROM PASTE TO INJECTABLE FORMULATION

Maria Francesca Di Filippo[a1], Luisa Stella Dolci[b1], Beatrice Albertini[b], Nadia Passerini[b], Paola Torricelli[c], Annapaola Parrilli[c], Milena Fini[c], Francesca Bonvicini[d], Giovanna Angela Gentilomi[e], Silvia Panzavolta[a]*, Adriana Bigi[a]

[a)]Department of Chemistry "G. Ciamician", University of Bologna, Via Selmi 2, 40126, Italy;

[b)] Department of Pharmacy and Biotechnology, University of Bologna, Via S. Donato 19/2, 40127, Italy;

[c)]IRCCS Istituto Ortopedico Rizzoli,Via di Barbiano 1-10, 40136, Bologna Italy;

[d)] Department of Pharmacy and Biotechnology, University of Bologna, Via Massarenti 9, 40138, Bologna;

[e)] Department of Pharmacy and Biotechnology, University of Bologna; Microbiology Unit, St Orsola-Malpighi University Hospital, Via Massarenti 9,40138 Bologna, Italy.

* corresponding author silvia.panzavolta@unibo.it

[1] these authors equally contributed to this work

Abstract

The development of infections still represents a severe problem in orthopedic field. In this work, we developed an anti-microbial and radiopaque calcium phosphate bone cement with a long-lasting inhibitory activity thanks to the addition of gentamicin sulphate-loaded solid lipid microparticles obtained by spray congealing. Cements containing gentamicin both added into cement powder and loaded into microparticles were prepared and characterized and their properties were compared. The results of structural, morphological, mechanical and in vitro characterizations indicate that inclusion of gentamicin into microparticles is a good approach in order to obtain materials able to display a strong inhibition towards the growth of Gram-negative, as well as Gram-positive bacteria and to enhance the viability of osteoblast-like cells.

All the compositions have an excellent activity also against clinical isolates, including multi drug resistant phenotypes. In particular, cements containing gentamicin-loaded microparticles display a strong and long-term inhibitory activity. Suitable modification of the liquid/powder ratio provided injectable formulation, whereas addition of $BaSO_4$ produced radiopacity. All the formulations display good injectability and cohesion, and no evidence of demixing.

Keywords: B. X-rays methods; C. Mechanical properties; D. Apatite; E. Biomedical applications.

1. Introduction

The development of calcium phosphate cements (CPCs) by Chow and Brown in the early 80 [1] led to a remarkable expansion of the possible applications of calcium phosphates-based biomaterials. CPCs are indeed biocompatible, bioactive and osteogenic systems [2-3], which are obtained by mixing a powder with a liquid phase to get a workable paste that hardens into a solid phase [3-5]. Bone cements are supposed to be subject to biological degradation and concomitant replacement by bone tissue. However, the degradation of CPCs *in vivo* is very slow [6], due to the low solubility of hydroxyapatite and to the limited extent of porosity of these materials [7], which is usually at the nanolevel and not sufficient to obtain the ingrowth of the tissue [8]. The properties of CPCs can be improved through enrichment of their composition with a variety of additives [3, 9-19]. Moreover, they can be utilized as drug delivery systems [11-13]. CPCs applications in bone replacement imply risks of infections due to bacterial colonization [14]. It follows that the addition of antibiotics to CPCs composition is of outmost interest, as testified by the high number of studies reported in the literature [2, 15-16]. The loading of the antibiotic

molecule is generally performed by adding it directly to the solid or to the liquid phase of the cement, even if this method has adverse effects on mechanical and setting properties of the cements, thus limiting the amount of drug that could be added [2,11]. The addition to the cement of poly(lactic-co-glycolic-acid) microspheres as antibiotics carriers has been proposed as a strategy to better control drug release and increase its bioavailability [17-18]. In previous papers, we demonstrated that spray-congealed solid lipid microparticles can be used to load an anti-osteoporotic drug, namely alendronate, into cements [19-20], in order to get systems able to stimulate bone formation, suppress bone resorption and prevent the lengthening of setting times and worsening of mechanical properties caused by the direct loading of the drug into cement composition [21-22]. Lipids display a favorable biocompatibility and lower toxicity compared with many polymers. Furthermore, the higher degradability of Cutina with respect to PLGA could favor the development of a microporosity inside the set cements [19-20]. In this paper, we explored the possibility to employ solid lipid microparticles obtained from Cutina to load an antibiotic into a biomimetic calcium phosphate cement in order to obtain a material able to sustain a potent antibacterial activity over a long period, and avoid the adverse effect of drug direct addition to the starting powders, as a delay of setting times and a decay of mechanical performances [11]. Gentamicin sulphate was chosen as model drug, since it is the utmost used agent for the treatment of severe infections caused by Gram positive (*Staphylococcus spp*.) and Gram-negative bacteria. The effect of the drug on the cement properties was investigated in cements where gentamicin sulfate was (i) loaded directly into the cement powder, (ii) loaded into the solid lipid microparticles, which were added to the cement, and (iii) loaded both directly into the cement powder and into the solid lipid microparticles. Moreover, barium sulfate was added as radiopacifying agent to the composition of cements, in order to allow the material to be

monitored during the surgery. The mechanical and structural properties of the cements were investigated as a function of the composition, in order to select the materials for cytotoxicity and antibacterial assessment. In particular, the antibacterial activity was tested *in vitro* against a panel of Gram-positive and Gram-negative reference bacterial strains and against a panel of clinical isolates recovered from patients with chronic bone or prosthetic joint infections. Finally, the conditions of preparation were optimized in order to use these systems as injectable bone cements.

2. Materials and Methods

2.1 Production of Cutina microparticles (MPs) and Gentamicin-loaded Cutina Microparticles (MPsGS) by Spray Congealing

Cutina® HR (hydrogenated castor oil) was purchased from Farmalabor S.R.L., Italy. Microparticles made of Cutina® HR (MPs) were produced by the spray-congealing process, as previously reported [19-20]. In order to prepare microparticles containing 20% wt of Gentamicin sulfate (MPsGS), the proper amount of GS (purchased by Carlo Erba, Italy) was slowly added under stirring to the melted Cutina to obtain a homogeneous suspension, which was then subjected to atomization. Obtained MPs were collected, sieved (range 75-250 μm) and stored in polyethylene closed bottles at 4 ± 2°C.

MPs and MPsGS were characterized as reported in S.I.

2.1.1 Evaluation of drug content

The drug content was measured by a spectrophotometric method, reported in literature and properly modified [23], that requires the use of Ninhydrin as derivatizing agent. The method was fully described in the S.I. section.

The samples were analyzed in duplicate and the encapsulation efficiency (EE) calculated as follows:

$$EE\ (\%) = (Wa/\ Wt) \cdot 100$$

where Wa was the actual drug content and Wt the theoretic one.

2.1.3 Evaluation of drug release from MPsGS

The GS release kinetic from MPsGS was measured as follows: 15 mg of MPsGS were accurately weighted and added to test tubes with 5 mL of PBS pH 7,4. Tubes were kept at 37°C and the solution was completely filtered after predetermined time intervals (15, 30, 60, 120, 180, 240 and 300 min) using a syringe with a straw equipped with 8 μm filter. The same amount of fresh buffer solution was replaced every time in each tube. The analysis was carried out in duplicate. GS content in filtered solution was evaluated by means of Ninhydrin derivatization, as reported above. GS powder (5 mg/5 mL of PBS pH 7,4) was used as reference.

2.2 Cement preparation

Dicalcium Phosphate Dihydrate (DCPD, $CaHPO_4 \cdot 2H_2O$), Barium sulphate ($BaSO_4$) and α-tricalcium phosphate (α-TCP) were synthesized following the procedure reported in literature [21]. Starting cement powders, made of gelatin and α-TCP (15% wt of gelatin with respect to the total amount) were prepared as previously reported [22]. 25 mg of DCPD ($CaHPO_4 \cdot 2H_2O$) were added to 475 mg of the gelatin/α-TCP mix powder, packed in a Teflon mold (6x12 mm) and mixed in an electric mortar (3M ESPE RotoMix) two times for 20 s. A liquid to powder ratio of 0.24 mL/g was used with distilled water as liquid phase. After addition of the liquid phase,

cement powders were mixed in the electric mortar two times for 20 s to obtain a paste of workable consistency and compacted for 1 min inside the Teflon mold by using a 4465 Instron dynamometer set at 70 N. After 10 min from the compaction, cement samples were demolded and immersed in PB at 37°C and pH 7.4 up to 21 days. These cements were used as control and labeled C.

For the preparation of cements enriched with different additives (GS and/or BaSO4 and/or MPs and/or MPsGS) the same procedure was followed, maintaining the same amounts of starting cement powders. The amount of each additive was calculated with respect to the weight of the starting powders and was added before mixing with the liquid phase. The cement compositions and the corresponding labels are reported in Table 1.

Table 1. Composition and labels of the cement pastes. The numbers indicate the amount of each additive in the formulation, expressed as weight %.

Label	**%$BaSO_4$**	**% GS**			**%MPs**	**%MPsGS**
	10	**2**	**4**	**8**	**10**	**10**
C_GS2		✓				
C_GS 4			✓			
C_GS 8				✓		
C_Ba	✓					
C_Ba_GS2	✓	✓				
C_Ba_GS 4	✓		✓			
C_Ba_GS 8	✓			✓		
C_MPs					✓	
C_MPsGS						✓
C_Ba_MPs	✓				✓	
C_Ba_MPsGS	✓					✓
C_Ba_GS2_MPsGSs	✓	✓				✓

2.3 Preparation of injectable cements

In order to obtain cement pastes of flowable consistency, the liquid to powder ratio for each composition was refined (see Table S4). The cements were prepared as described above and samples were labeled as reported in Table 2.

Table 2. Composition and labels of the injectable cements.

Label	$BaSO_4$	GS 2	MPs	MPsGS
in_C_Ba	✔			
in_C_Ba_GS2	✔	✔		
in_C_Ba_MPs	✔		✔	
in_C_Ba_MPsGS	✔			✔
in_C_Ba_GS2_MPsGS	✔	✔		✔

3. Characterization

3.1 Setting times determination

Initial and final setting times were determined by the Gillmore method (ASTM, American Society for Testing and Materials: C 266- 89. Standard test method for time of setting of hydraulic cement paste by Gillmore needles). Measurements were performed at 37°C for the injectable composition and at RT for the pastes.

3.2 X-Ray Powder Diffraction

For X-ray investigations, the samples were removed from PB after different soaking times, immediately immersed in liquid nitrogen for few minutes in order to stop the hardening reaction, dried at 37°C for one night and then ground in a mortar. X-ray powder diffraction analyses were carried out by means of a Philips X'Celerator powder diffractometer equipped with a graphite monochromator in the diffracted beam. CuKα radiation (λ= 1,54 Å; 40 mA, 40 kV) was used.

The diffraction patterns were obtained in the 3- 50°/ 2θ range using a 0,03 step and a 3°/min speed. The relative amount of α-TCP conversion into calcium-deficient hydroxyapatite (CDHA) was determined through Rietveld refinement of powder diffraction patterns.

3.3 Mechanical tests in compression

Mechanical properties after different soaking times in PB, were evaluated on cylindrical specimens (6 mm in diameter, 12 mm in length) using a 4465 Instron dynamometer equipped with a 1 kN load cell. Stress-strain curves were recorded at a crosshead speed of 1 mm/min by the software SERIE IX for Windows.

At least 6 specimens for each incubation time were tested. Two-ways analysis of variance (ANOVA) followed by Bonferroni's Multiple comparison test was employed to assess statistical significance of the experimental conditions; statistically significant differences were determined at $p < 0.05$.

3.4 Micro-CT characterization

In order to obtain a quantitative and tridimensional analysis of cement's porosity, selected samples (C_Ba, C_GS2, C_MPsGS and C_Ba_GS2_MPsGS after 21 days of soaking in PB solution) were scanned using a high-resolution micro-CT SkyScan 1172 (Bruker Micro-CT, Kontich, Belgium). The voltage source and the current were set at 100 kV and 100 μA respectively, using a Cu/Al filter and with a nominal resolution of 6,5 μm (pixel dimension). Micro-tomographic sections were obtained and then used to measure the overall porosity and create virtual 3D model of the analyzed object which allows realistic visualizations of the sample in the space, as reported in S.I.

3.5 Evaluation of injectability and cohesion

The injectability and cohesion of the CPCs were determined as reported in S.I

3.6 Antibacterial activity

3.6.1 Bacterial strains and Kirby-Bauer method

The antibacterial activity of disk-shaped samples C_Ba, C_Ba_GS2, C_Ba_MPs, C_Ba_MPsGS and C_Ba_GS2_MPsGS was evaluated in vitro against a panel of defined control strains from the American Type Culture Collection (ATCC) including three Gram positive bacterial strains (*Staphylococcus aureus* ATCC 25923, *Staphylococcus epidermidis* ATCC 12228, *Enterococcus faecalis* ATCC 29212) and three Gram negative bacterial strains (*Escherichia coli* ATCC 25922, *Pseudomonas aeruginosa* ATCC 27853, *Klebsiella pneumoniae* ATCC 9591). In addition to these selected test organisms, 20 clinical isolates recovered from patients with chronic bone or prosthetic joint infections, and collected at the Microbiology Unit, St Orsola Malpighi University Hospital (Bologna, Italy) were used in the present study. Clinical strains were isolated on BD Columbia Agar with 5% sheep blood (Becton Dickinson, GmbH, Germany) and confirmed by MALDI-TOF MS (BrukerDaltonik, GmbH, Germany) (Croxatto, A 2012). Their antibiotic susceptibility was determined by using the Vitek2 semi-automated system (bioMerieux, France) and interpreted following EUCAST guidelines (EUCAST). For the Kirby-Bauer (KB) disk diffusion assay, the surface of Mueller-Hinton (MH) agar plate (Sigma-Aldrich) was inoculated with the bacterial suspension at 0.5 McFarland, and sterilized disks (Ø = 6.0 mm) were placed on the agar plates. As control, gentamicin disk (GMN 10 μg) was included in each assay. After 24 hours of incubation at 37°C the agar plate was observed and the inhibition zone diameters (corresponding to the bacterial-free zone around the disk-shaped sample) was measured to the nearest whole millimeter with a ruler. All experiments were performed on duplicate in different days. One-way analysis of variance (ANOVA) followed by Turkey's multiple comparison test

was used to compare the antibacterial properties among samples. Differences were considered statistically significant with $p < 0.05$.

3.6.2 Antibacterial activity over the time on *S. aureus* ATCC 25923

Selected disk-shaped samples, C_Ba_GS2, C_Ba_MPsGS and C_Ba_GS2_MPsGS, were assayed for their antibacterial activity towards *S. aureus* ATCC 25923 over a long period of incubation in PB solution, at pH 7.3 and at 37°C to mimic physiological environment, as reported in S.I.

3.7 Cytotoxicity tests

Human osteoblast-like cells MG63 (OB, Istituto Zooprofilattico Sperimentale IZSBS, Brescia, Italy), were cultured in DMEM medium (Dulbecco's Modified Eagle's Medium, Sigma, UK) supplemented with 10% FCS and antibiotics (100 U/ml penicillin, 100 μg/ml streptomycin). Cells were detached from culture flasks by trypsinization and cell number and viability were checked by erythrosine B dye. OB cells were plated at a density of 3x104 cells/ml in 24-well plates containing six sterile samples of the following biomaterial: C_Ba, C_Ba_MPsGS, C_Ba_GS2, C_Ba_GS2_MPsGS. Cells were also plated in wells for negative (CTR–, DMEM only) and positive (CTR+, DMEM + 0.05% phenol solution) controls. Plates were cultured in standard conditions, at 37 ± 0.5°C with 95% humidity and 5% ± 0.2 CO_2 up to 72 hours.

The quantitative evaluation of cytotoxicity was performed by measuring cell viability and lactate dehydrogenase enzyme (LDH) release, whereas cell morphology was performed by Live/Dead® assay (Molecular Probes, Eugene, OR, USA), as reported in S.I.

4. Results

4.1 Production and characterization of MPs and MPsGS

Cutina HR microparticles containing or not 20% wt of GS (MPs and MPsGS) were prepared as described in Materials and Methods. Both MPs and MPsGS present a Gaussian dimensional distribution with a maximum centered at about 100-150 μm (Figure 1a). Evaluation of encapsulation efficiency of GS confirmed the theoretical value of 20% and did not reveal any significant difference as a function of particles size, as shown in Figure S1. For this reason, the size fraction included in the cement's formulation was that corresponding to 100-150 μm. MPsGS appeared round-shaped and exhibited almost smooth surfaces, although small pores were appreciable on the particles surface (see Figure 1b).

X-ray diffraction pattern of GS powder showed a very broad halo centered at about 20°/2 theta, whereas the patterns of MPsGS displayed several diffraction reflections, in particular two peaks centered at 5.2, 19.5 and 21.95°/2 theta, characteristic of Cutina (Figure S2).

The DSC curve of MPsGS showed both Cutina and GS peaks at 90°C (Cutina melting point) and at 250 °C (GS melting decomposition), respectively [24], suggesting that the spray congealing process did not modify the solid state of the drug and of the carrier (Figure S2). Hot Stage microscopy (HSM) showed clear evidence of the presence of GS after fusion of the low-melting excipient (see Figure S3). Figure S4 reports the GS released from MPsGS as a function of soaking time in PB: as expected, encapsulation of GS into lipid microparticles led to a prolonged release over time. In fact, due to the high solubility of GS, when the powder is put in aqueous medium, its dissolution is nearly instantaneous and after 15 minutes the GS was completely recovered, while the release from MPs is completed only after 5 hours6.

4.2 Cement pastes loaded with GS and/or $BaSO_4$

The effect of GS and/or barium sulphate on the mechanical, setting and hardening behavior of the cement pastes was evaluated. Mechanical properties in compression were tested after 7 and 21 days of soaking in PB and the values of maximum stress, obtained from the stress-strain curves, as well as the initial and final setting times, are reported in Table S1, while the effect of both the additives on the hardening reaction was evaluated through X-ray diffraction analysis. Figure 2 reports, as an example, the XRD patterns recorded on C_Ba cements after different soaking times, compared to $BaSO_4$ pattern.

The presence of $BaSO_4$, added in order to obtain a radiopaque material [25-26], seems to elicit a negligible delay in the conversion reaction: after 21 days the most intense reflection of a-TCP is barely appreciable. A quantitative evaluation of the extent of conversion of a-TCP into hydroxyapatite as a function of soaking time was performed by means of Rietveld analysis of each pattern. The results are summarized in Table S2. Higher amounts of GS have a negative effect on the material properties, decreasing mechanical performances, slowing down the hardening reaction and lengthening both initial and final setting times, in tune with data reported in literature [11]. Concurrent addition of $BaSO_4$ limits this negative trend: however, it is evident that direct addition of GS to the powders must be limited to a value of 2% wt, in order to maintain cement properties. On this basis, further investigations were carried out using only one percentage of GS (2% wt), both when loaded into MPs and when directly added to the cement powders.

4.3 Cement pastes containing MPs and MPsGS

Inclusion of MPs is an effective method to incorporate drugs or bioactive molecules into cement pastes without affecting cement properties [7, 19-20]. Values of maximum stress under

compression and initial and final setting times of MPs-containing cements are reported in Table 3, together with those of C samples for comparison. As desirable, the compressive strength of C_MPs and of C_MPsGS was not significantly different ($p > 0.05$) thus confirming that the loading of GS into the microspheres did not modify the mechanical properties of the resulting cements (2way-ANOVA with Bonferroni post-tests). Table 4 reports the extent of hydroxyapatite obtained from α-TCP conversion after different soaking times: the complete conversion of C cements took place after 7 days of soaking in PB, while in the presence of both MPs and MPsGS, the hardening reaction slowed down and the conversion was obtained after 21 days.

Furthermore, with the aim to enhance the total amount of GS without worsening the cement properties, a 2% wt of GS powder was added to the formulation containing MPsGS and barium sulphate (sample C_Ba_GS2_MPsGS). This addition did not affect the setting times and provoked just a slight reduction of the mechanical properties at 7 days, probably due to the lengthening of the hardening reaction (**$p < 0.01$ C_MPs vs C_Ba_GS2_MPsGS), but no significant differences were observed at 21 days (see Tables 3 and 4).

Table 3. Mechanical properties (compressive strength) and setting times (initial and final) of the cements containing different additives. Values are the mean ± standard deviation of at least 6 samples (**$p < 0.01$ C_MPs vs C_Ba_GS2_MPsGS; [a]$p > 0.05$)

Sample	**σ_{max} (MPa) 7d**	**σ_{max} (MPa) 21d**	**t_i (min)**	**t_f (min)**
C	10.1 ± 0.6	15 ± 1	6 ± 1	13 ± 3
C_MPs	12 ± 2 **,[a]	10.2 ± 0.1	5 ± 1	11 ± 3
C_MPsGS	10 ± 1	10 ± 1	4 ± 1	7 ± 2
C_Ba_MPs	15 ± 5	13 ± 1	4 ± 2	6 ± 3
C_Ba_MPsGS	10 ± 1[a]	10 ± 2	4 ± 2	6 ± 3
C_Ba_GS2_MPsGS	5.0 ± 0.5**	8 ± 2	4 ± 2	6 ± 3

Table 4. Relative amount (%) of hydroxyapatite of the cements after different soaking times in PB. Values were obtained by Rietveld refinement of the powder X-ray diffraction patterns.

Sample	7d	21d
C	100	100
C_MPs	90	100
C_MPsGS	89	97
C_Ba_MPs	65	80
C_Ba_MPsGS	60	80
C_Ba_GS2_MPsGS	40	70

4.4 Micro-CT characterization

To get some insights on the cement's texture due to the influence of the additives, micro-CT analysis was carried out on the samples C_Ba, C_GS2, C_MPsGS and C_Ba_GS2_MPsGS. 3D models of representative samples analyzed by micro-CT are reported in Figure 3.

Due to the voltage set of micro-CT used for data acquisition of the composite cements, MPs and MPsGS resulted radiotransparent: this implies that part of the porosity detected in the samples may actually be constituted also by microparticles.

In fact, together with a microporosity due to the cement structure, 2D distribution of pores size, ~~reported in Figure 4,~~ highlights a higher percentage of "porosity" of size between 0.1 and 0.2 mm in MPs- and MPsGS- containing cements (the main size of added microparticles, measured through SEM images, see Figure 1).

The values of total porosity (%) of C_MPsGS and C_Ba_GS2_MPsGS, reported in Table 5, are indeed higher than those found for C_Ba and C_GS2, thus confirming this hypothesis.

Table ~~4~~. 3D morphometric analysis of porosity detected by micro-CT acquisition of representative cements.

Samples	P.tot (%)
C_Ba	3.35

C_GS2	3.88
C_ MPsGS	10.55
C_Ba_GS2_MPsGS	22.60

4.5 Cytotoxicity assessment

Sample C_Ba, C_Ba_GS2, C_Ba_MPsGS and C_Ba_GS2_MPsGS were selected in order to evaluate the influence of each additive on the biological and antibacterial properties of the cements. LDH dosage (Figure 4a) is an indirect parameter of cytotoxicity, because its release in culture medium is due to a damage of cell membranes. The test showed low values of LDH, not different from CTR−, for all samples. All values were significantly lower when compared to CTR+ ($p<0.0005$).

Cell viability was performed after 72 hours of culture (Figure 4b). No signs of cytotoxicity were shown, as demonstrated by values of WST1 test, which do not differ (C_Ba_GS2_MPsGS) or are even significantly higher (C_Ba, C_Ba_MPsGS, C_Ba_GS2, $p<0.005$) than CTR−. Moreover, cells were stained with Live&Dead fluorescent staining for qualitative evaluation of cell morphology (Figure 4c): all the samples showed good colonization of surface with cells displaying a normal morphology (green staining). As expected, CTR+ showed a significant reduction in viability and images confirmed the presence of numerous dead cells (red staining).

4.6 Antibacterial activity

The antibacterial properties of the cements C_Ba, C_Ba_GS2, C_Ba_MPsGS and C_Ba_GS2_MPsGS were evaluated by a KB diffusion assay towards a set of control strains and

a panel of clinical isolates characterized for their susceptibility profile by standard procedures (EUCAST testing guidelines). C_Ba_MPs was added as a further control. As reported in Table 6, all disk-shaped biomaterials containing GS inhibited bacterial growth as a clear bacterial free-zone was measured around disks following incubation. On the contrary, C_Ba and C_Ba_MPs did not determine inhibition confirming the reliability of the sample preparation and testing procedure.

Table ~~5.~~ Antibacterial activity of the cements. Median values and ranges of the inhibition zone diameters (in millimeter) against ATCC control strains are reported.

Sample	***S. aureus*** **(ATCC 25923)**	***S. epidermidis*** **(ATCC 12228)**	***E. faecalis*** **(ATCC 29212)**	***E. coli*** **(ATCC 25922)**	***K.pneumoniae*** **(ATCC 9591)**	***P. aeruginosa*** **(ATCC 27853)**
C_Ba	NA[a]	NA	NA	NA	NA	NA
C_Ba_GS2	21 (20-22)	26.5 (26-27)	14 (13-15)	19.5 (19-20)	22 (21-23)	23.5 (23-24)
C_Ba_MPs	NA	NA	NA	NA	NA	NA
C_Ba_MPsGS	22.5 (22-23)	28.5 (27-30)	15	19.5 (19-20)	21.5 (21-22)	23.5 (23-24)
C_Ba_GS2_MPsGS	25.5 (25-26)	29 (28-30)	17 (16-18)	21 (20-22)	24 (23-24)	25 (24-26)
GMN[b]	18.5 (18-19)	24 (23-25)	9	18	18 (17-19)	17

[a] NA, not appearing.
[b] GMN, disk containing 10 μg of gentamicin and used as positive control.

For a fully characterization of the antibacterial potential, C_Ba_GS2, C_Ba_MPsGS and C_Ba_GS2_MPsGS were assayed against 20 clinical isolates of *S. aureus and S. epidermidis*, including multidrug-resistant *Staphylococci*, and the results are reported in Table 7.

Table ~~6.~~ Antibacterial activity of the cements. Median values and ranges of the inhibition zone diameters (in millimeter) against clinical strains are reported.

Sample	***MSSA***[a] ***(n = 5)***	***MRSA***[b] ***(n = 5)***	***MSSE***[c] ***(n = 5)***	***MRSE***[d] ***(n = 5)***
C_Ba_GS 2	29.5 (28-32)	26 (26)	34 (33-35)	31 (26-31)
C_Ba_MPsGS	29.5 (29-32)	26.5 (26-28)	34 (33-35)	31.5 (28-34)

C_Ba_GS2_MPsGS	32 (31-34)	28 (27-29)	36.5 (36-37)	34 (30-36)
GMN[e]	22.5 (22-23)	21 (19-22)	29 (28-30)	26.5 (22-28)

[a]methicillin-sensitive *S. aureus* strains; [b]methicillin-resistant *S. aureus* strains; [c]methicillin-sensitive *S. epidermidis* strains; [d]methicillin-resistant *S. epidermidis* strains; [e] GMN, disk containing 10μg of gentamicin and used as positive control.

The three biomaterials displayed strong antibacterial properties against all tested clinical isolates and, comparing the diameters of the inhibition zones, a significantly greater activity of C_Ba_GS2_MPsGS respect to C_Ba_GS2 andC_Ba_MPsGS was observed for methicillin-sensitive *S. aureus* strains (C_Ba_GS2 vs C_Ba_GS2_MPsGS**: $p<0.001$; C_Ba_MPsGS vs C_Ba_GS2_MPsGS*: $p<0.05$).

These bacterial strains were chosen to represent a spectrum of pathogens associated with joint and bone infections, as resistance to antibiotics is one of the mayor concerns in antimicrobial therapy. The antibiotic-resistance profile of each clinical strain is reported in Table S3.

4.6.1 Antibacterial activity over time

In order to correlate the antibacterial activity over time to the cement's composition, GS containing cements (C_Ba_GS2, C_Ba_MPsGS and C_Ba_GS2_MPsGS) were put in PB solution and withdrawals assessed towards *S. aureus* control strain.

The liquid samples recovered after different incubation times were diluted 1:500 and incubated with the inoculum suspension at 37°C for 24 h. Thereafter bacterial growth was spectrophotometrically measured at 630 nm and inhibition was calculated relative to the positive control. Figure 5 reports bacterial growth inhibition as a function of incubation times. Up to the forth recovery of PB solution, the GS released from the three materials inhibit *S. aureus* growth at the same extent, while at later sampling the antibacterial activity of GS from C_Ba_MPsGS and C_Ba_GS2_MPsGS was significantly higher compared to C_Ba_GS2.

The effectiveness of GS loaded as powder from C_Ba_GS2 samples gradually decreased with time, down to negligible levels (6.5%) at 21 days. On the contrary, GS from MPs displayed a strong and long-term inhibitory activity in both formulations (78.0% and 68.6% for C_Ba_MPsGS and C_Ba_GS2_MPsGS, respectively). The excellent and prolonged activity of the biomaterials containing MPs was confirmed by KB diffusion assay performed with the cement disk recovered after 21 days of soaking. While the median value of the inhibition zone diameter obtained for C_Ba_GS2 was only 14 mm, for C_Ba_MPsGS and C_Ba_GS2_MPsGS it was 18 mm, suggesting that these biomaterials maintained high inhibitory properties over a long period. Overall these results confirm the suitability of the multicomposite system for local application in the treatment of orthopedic chronic infections.

4.7 Injectable CPC formulation

Injectability of CPC is an important feature for minimally invasive surgical techniques, in applications involving defects with limited accessibility and narrow cavities and when there is the need to conform to a defect area of complex shape [27]. Injectable formulations were obtained by suitable adjustment of the L/P ratio: the compositions and the added volumes of water are summarized in Table 8, which also reports the values of setting times measured at 37°C.

Table ~~7~~. Liquid to powder ratios and setting times of injectable cements.

Sample	**Liquid/Powder (mL/g)**	**Setting times (min)**	
in_C_Ba	0,55	t_i= 24± 3	t_f = 38± 2
in_C_Ba_GS 2	0,60	t_i = 22± 3	t_f = 37± 2
in_C_Ba_MPsGS	0,65	t_i = 18± 3	t_f = 34± 2

in_C_Ba_GS 2_MPsGS	0,65	t_i = 18± 3	t_f = 33± 2
in_C_Ba_GS 2_MPsGS	0,75	t_i = 19± 3	t_f = 35± 2

The injectable cements presented good injectability (as demonstrated in Figure 6a, recorded during extrusion and in Video 1) and an excellent cohesion as observed in PB solution immediately after extrusion (Figure 6b) and after one day of storing (Figure 6c). In order to get some information about the hardening reaction, X-ray diffraction patterns were collected on cements after different times of soaking. Figure S5 shows patterns collected on cements of different formulations after 1 day of soaking in PB.

Furthermore, we collected the material at different times during the extrusion and performed an accurate morphological observation along the wire length by means of scanning electron microscopy. From the images recorded for sample in_C_Ba_MPs and reported in Figure 7, it can be inferred that the MPs are regularly distributed along the whole length of the wire, thus confirming their good dispersion and the absence of phase separation during injection.

Injectability curves (Figure 8) were registered recording the injection force as a function of the plunger displacement, in order to assess the ease of injection. A very rapid increase of the load in the first millimeters of displacement is due to the critical force that must be applied to start the flow of the paste, while the subsequent plateau (in the absence of phase separation) is related to the load needed to maintain the flow. In the last portion of the curves, the load increases abruptly because of the mechanical contact between the plunger and the syringe's bottom when all the paste has been extruded; hence, the system was stopped [28-32].

The introduction of MPs into cement's formulation decreases the injectability: more pressure was needed to extrude the paste from the syringe (see Figure 8a).

Sample in_C_Ba_GS2_MPsGS was tested using two different liquid to powder ratios (Figure 8b): the formulation at 0,75 mL/g provides a good injectability of the cement since the required load during the extrusion is about 300 N.

Radiopacity of C_Ba_MPsGS was demonstrated by the radiograph reported in Figure S6: the presence of barium sulphate allows easy detection of the cement.

5. Discussion

The results of this work demonstrate that Cutina solid lipid microparticles produced by a solvent free technique can be used as carriers of the antibiotic Gentamicin sulphate, in order to provide cement formulations with antibacterial properties, without worsening their mechanical properties. MPs, loaded with 20% wt of GS, were successfully obtained by spray congealing technology. In order to evaluate the influence of different additives on cement properties, $BaSO_4$, GS as powder, MPs and MPsGS were added separately, as well as in mixed compositions, to a weighted amount of cement powder.

The value of maximum stress of the control cement (C) increased as a function of time due to the hardening reaction. Direct addition of GS powder had a strong effect on both mechanical and setting properties of the cements (Table S1), as expected from the literature [11]. In fact, just the introduction of a 2% of GS provoked a reduction of the values of maximum stress in comparison to those obtained for C cements, at every experimental time. Moreover, the compressive strength of the materials decreased as the amount of GS increased, along with a lengthening of both initial and final setting times (see table S1). On the other hand, the addition of barium sulfate reduced the negative influence of GS on the mechanical properties without influencing the setting times (see Table S1).

The extent of conversion of a-TCP into hydroxyapatite, shown in Table S2, indicates that the cements loaded with 2 wt% of GS were almost totally converted after 7 days, suggesting that this amount of antibiotic does not greatly interfere with the hardening reaction. However, greater GS contents delayed the hardening reaction thus justifying the worsening of the mechanical properties observed on increasing GS content [11].

The mechanical properties of the cements containing MPs were not significantly different from those of the cements containing MPsGS ($p > 0.05$), thus confirming the effectiveness of the proposed method [18]. Only the cements containing both free GS and drug-loaded MPs displayed a significant worsening of the compressive strength at 7 days compared with C_MPs, even though initial and final setting times were not significantly influenced by the presence of the additives.

Moreover, the addition of MPs, as well as of barium sulfate, had a minor effect on the process of conversion of α-TCP into hydroxyapatite, whereas the simultaneous addition of the two additives delayed the conversion, which is further slowed down by the presence of GS powder (see Table 4). A demonstration of the absence of any cytotoxic effect (a reduction of viability by more than 30% is considered a cytotoxic effect) relies in the values of proliferation (expressed as percentage relative to CTR-), which were all over the limit of 70%, and was confirmed by LDH values and cell morphology (Figure ~~5~~).

The antibacterial properties were at first evaluated by means of KB method: although no significant differences were appreciated in Gram negative bacteria, the median values of the inhibition zone diameters obtained for Gram positive strains on cements containing MPsGS were higher than those measured for samples containing GS loaded directly into cement composition (see Table 6). Considering that C_Ba_GS and C_Ba_MPsGS contain the same drug amount, it is

possible to speculate that lipid microparticles enhance GS uptake through the bacterial membrane. Furthermore, the biomaterials C_Ba_GS2, C_Ba_MPsGS and C_Ba_GS2_MPsGS displayed strong antibacterial properties also against all the tested clinical isolates. As expected, the comparison of the median values of the inhibition zones (Table 7) revealed that the multisystem biomaterial C_Ba_GS2_MPsGS displayed the greatest inhibitory activity towards all bacterial strains as consequence of the additive effect of GS powder and GS-loaded MPs.

More information was obtained by evaluating antibacterial activity over the time on S. aureus. Up to 3 days, the inhibition of *S. aureus* growth was the same for the three materials, while at longer times the antibacterial activity of C_Ba_MPsGS and C_Ba_GS2_MPsGS was significantly higher compared to C_Ba_GS2 (see Figure ~~6~~). Moreover, the effectiveness of C_Ba_GS2 gradually decreased with time down to negligible levels (6.5%) at 21 days, while GS from MPs displayed a strong and long-term inhibitory activity in both formulations.

These results suggest that both the composite biomaterials, C_Ba_MPsGS and C_Ba_GS2_MPsGS could be really effective in the treatment of bacterial infections, combining a potent initial antibacterial action with a sustained release over time, which is an important feature to avoid the administration of insufficient doses of drug, which can lead to the arising of antibacterial resistances.

All the formulations could be employed to realize injectable cements through a simple modification of the liquid to powder ratio. The results of the injectability tests indicate that the optimized L/P ratios ensure good injectability [28] for all the compositions, as shown in Figure ~~7~~a and in Video 1. The results of the cement cohesion were also very satisfying: when injected into saline solution immediately after extrusion, the CPC paste maintained its wire-like shape until hardening, with no sign of disintegration during the process (Figure ~~7~~b). The cement

maintained a good cohesion even after 24 hours and exhibited a highly homogeneous dispersion of MPs inside the extruded wire. In particular there was no evidence of phase separation, which is a major issue inhibiting successful delivery of injectable CPC.

6. Conclusions

The results of this study allowed to develop anti-bacterial and radiopaque calcium phosphate cements, which can be turned from non-injectable to fully injectable by simple variation of liquid to powder ratio. Thanks to the use of spray congealed microparticles, gentamicin sulfate can be added to the cement composition without the lengthening of the setting times and the worsening of the compressive strength observed when the drug is loaded directly into the cement powder without the protection of the MPs. Human osteoblast-like cells displayed a good viability on all the examined cement formulations. Moreover, all the compositions exhibited a strong inhibitory activity towards Gram positive and Gram-negative reference bacterial strains and clinical isolates. In particular, cements with gentamicin loaded MPs showed an enhanced inhibition towards Gram-positive bacteria and a sustained release of the drug which provides a long-term antibacterial activity, fundamental in the treatment of chronicle infections. Injectable formulations displayed good injectability, high cohesion and good dispersion of MPs into the extruded cements without any phase separation.

Supporting Information Available

References

(1) W.E. Brown, L.C. Chow, A new calcium phosphate water setting cement. In: Brown, P.W. (Eds.), Cements Research Progress, Westerville, OH: American Ceramic Society, 1986, pp. 352–379.

(2) M.P. Ginebra, M. Espanol, E.B. Montufar, E.A. Perez, G. Mestres, New processing approaches in calcium phosphate cements and their applications in regenerative medicine, Acta Biomater., 6 (2010) 2863–2873. https://doi.org/10.1016/j.actbio.2010.01.036’’\h

(3) J. Zhang, W. Liu, V. Schnitzler, F. Tancret, J.M. Bouler, Calcium phosphate cements for bone substitution: Chemistry, handling and mechanical properties, Acta Biomater.**,** 10 (2014) 1035–1049. https://doi.org/10.1016/j.actbio.2013.11.001.

(4) M. Bohner, Reactivity of calcium phosphate cements, J. Mater. Chem., 17 (2007) 3980–3986. https://doi.org/10.1039/B706411J.

(5) S.V. Dorozhkin, Self-setting calcium orthophosphate formulations, J.Funct. Biomater., 4 (2013) 209-311. https://doi.org/10.3390/jfb4040209.

(6) E.M. Ooms, J.G. Wolke, J.P. van der Waerden, J.A. Jansen, Trabecular bone response to injectable calcium phosphate (Ca–P) cement, J. Biomed. Mater. Res., 61 (2002) 9–18. https://doi.org/10.1002/jbm.10029.

(7) R.P. Félix Lanao, S.C.G. Leeuwenburgh, J.G.C. Wolke, J.A. Jansen, Bone response to fast-degrading, injectable calcium phosphate cements containing PLGA microparticles, Biomater., 32 (2011) 8839-8847. https://doi.org/10.1016/j.biomaterials.2011.08.005.

(8) O. Acarturk, M. Lehmicke, H. Aberman, D. Toms, J.O. Hollinger, M. Fulmer, Bone Healing Response to an Injectable Calcium Phosphate Cement with enhanced radiopacity, J. Biomed. Mater. Res. B Applied Biomaterials, 86 (2008) 56-62. https://doi.org/10.1002/jbm.b.30987.

(9) A. Bigi, E. Boanini, Functionalized biomimetic calcium phosphates for bone tissue repair, J. Appl. Biomater. Func. Mater., 15(4) (2017), e313-e325. https://doi.org/ 10.5301/jabfm.5000367.

(10) A. Sugawara, K. Asaoka, S.J. Ding, Calcium phosphate-based cements: clinical needs and recent progress, J. Mater. Chem. B, 1 (2013**)** 1081-1089. https://doi.org/10.1039/C2TB00061J.

(11) M.P. Ginebra, C. Canal, M. Espanol, D. Pastorino, E.B. Montufar, Calcium phosphate cements as drug delivery materials, Adv. Drug Deliv. Rev., 64 (2012) 1090–1110. https://doi.org/10.1016/j.addr.2012.01.008.

(12) L. Kyllönen, M. D'Este, M. Alini, D. Eglin, Local drug delivery for enhancing fracture healing in osteoporotic bone, Acta Biomater., 11 (2014**)**, 412–434. https://doi.org/10.1016/j.actbio.2014.09.006.

(13) A. Bigi, E. Boanini, Calcium Phosphates as Delivery Systems for Bisphosphonates, J. Funct. Biomater., 9 (2018). https://doi.org/10.3390/jfb9010006.

(14) M.G. Kaufman, J.D. Meaike, S.A. Izaddoost, Orthopedic Prosthetic Infections: Diagnosis and Orthopedic Salvage, Semin. Plast. Surg., 30 (2016) 66–72. https://doi.org/10.1055/s-0036-1580730.

(15) U. Uskokovic´, S. Ghosh, W.M. Wu, Antimicrobial hydroxyapatite–gelatin–silica composite pastes with tunable setting properties, J.Mater. Chem. B, 5 (2017) 6065-6080. https://doi.org/10.1039/C7TB01794D.

(16) D. Pastorino, C. Canal, M.P. Ginebra, Drug delivery from injectable calcium phosphate foams by tailoring the macroporosity–drug interaction, Acta Biomater., 12 (2015) 250–259. https://doi.org/10.1016/j.actbio.2014.10.031.

(17) J. Schnieders, U. Gbureck, R. Thull, T. Kissel, Controlled release of gentamicin from calcium phosphate- poly(lactic acid-co-glycolic acid) composite bone cement, Biomater., 27 (2006) 4239–4249. https://doi.org/10.1016/j.biomaterials.2006.03.032.

(18) D. Loca, M. Sokolova, J. Locs, A. Smirnova, Z. Irbe, Calcium phosphate bone cements for local vancomycin delivery, Mater. Sci. Eng. C, 49 (2015) 106–113. https://doi.org/10.1016/j.msec.2014.12.075.

(19) L.S. Dolci, S. Panzavolta, B. Albertini, B. Campisi, M. Gandolfi, A. Bigi, N. Passerini, Spray-congealed solid lipid microparticles as a new tool for the controlled release of bisphosphonates from a calcium phosphate bone cement, Eur. J. Pharm. Biopharm., 122 (2018) 6–16. https://doi.org/10.1016/j.ejpb.2017.10.002.

(20) L.S. Dolci, S. Panzavolta, P. Torricelli, B. Albertini, L. Sicuro, M. Fini, A. Bigi, N. Passerini, Modulation of Alendronate release from a calcium phosphate bone cement: An in vitro osteoblast-osteoclast co-culture study, Int. J. Pharm., 554 (2019) 245-255. https://doi.org/10.1016/j.ijpharm.2018.11.023.

(21) S. Panzavolta, P. Torricelli, B. Bracci, M. Fini, A. Bigi, Alendronate and pamidronate calcium phosphate bone cements: Setting properties and in vitro response of osteoblast and osteoclast cells, J. Inorg. Biochem., 103 (2009) 101–106. https://doi.org/10.1016/j.jinorgbio.2008.09.012.

(22) S. Panzavolta, P. Torricelli, B. Bracci, M. Fini, A. Bigi, Functionalization of biomimetic calcium phosphate bone cements with alendronate, J. Inorg. Biochem., 104 (2010) 1099-1106. https://doi.org/10.1016/j.jinorgbio.2010.06.008.

(23) P. Frutos, S. Torrado, M.E. Perez-Lorenzo, G. Frutos, A validated quantitative colorimetric assay for gentamicin, J. Pharm. Biomed Anal., 21 (2000) 1149-1159. https://doi.org/10.1016/S0731-7085(99)00192-2.

(24) B.E. Rosenkrantz, J.R. Greco, J.G. Hoogerheide, M. Oden, Gentamicin. In: Florey, K. (Ed.), Analytical profile of a drug substances vol. 9. Orlando, USA: Academic Press, ISBN: 0122608267, (1980), pp. 295-340.

(25) M.P. Ginebra, L. Albuixech, E. Fernandez-Barragan, C. Aparicio, F.J. Gila, J. San Roman, B. Vazquez, J.A Planell, Mechanical performance of acrylic bone cements containing different radiopacifying agents, Biomater., 23 (2002) 1873–1882. https://doi.org/10.1016/s0142-9612(01)00314-3.

(26) C. Fang, R. Hou, K. Zhou, F. Hua, Y. Cong, J. Zhang, J. Fu, Y.I. Cheng, Surface functionalized barium sulfate nanoparticles: controlled in situ synthesis and application in bone cement, J. Mater. Chem. B, 2 (2014) 1264–1274. https://doi.org/10.1039/C3TB21544J.

(27) J. Jansen, E. Ooms, N. Verdonschot, J. Wolke, Injectable calcium phosphate cement for bone repair and implant fixation, Orthop. Clin. N. Am., 36 (2005) 89-95. https://doi.org/10.1016/j.ocl.2004.06.014.

(28) E.F. Burguera, H.K. Hockin, L. Sun, Injectable calcium phosphate cement: Effects of powder-to-liquid ratio and needle size, J. Biomed. Mater. Res. B, 84(2) (2008) 493-502. https://doi.org/10.1002/jbm.b.30896.

(29) W. Liu, J. Zhang, G. Rethore, K. Khairoun, P. Pilet, F. Tancret, J.M. Bouler, P. Weiss, A novel injectable, cohesive and toughened Si-HPMC (silanized-hydroxypropyl methylcellulose) composite calcium phosphate cement for bone substitution, Acta Biomater. 10 (2015) 3335–3345. https://doi.org/10.1016/j.actbio.2014.03.009.

(30) R. O'Neill, H.O. McCarthy, E.B Montufar, M.P. Ginebra, D.I.Wilson, A. Lennon, N. Dunne, Critical review: Injectability of calcium phosphate pastes and cements, Acta Biomater., 50 (2017) 1-19. https://doi.org/10.1016/j.actbio.2016.11.019.

(31) S. Tadier, L. Galea, B. Charbonnier, G. Baroud, M. Bohner, Phase and size separations occurring during the injection of model pastes composed of b-tricalcium phosphate powder,

glass beads and aqueous solutions, Acta Biomater., 10 (2014) 2259–2268. https://doi.org/10.1016/j.actbio.2013.12.018.

(32) M. Habib, G. Baroud, F. Gitzhofer, M. Bohner, Mechanism underlying the limited injectability of hydraulic calcium phosphate paste, Acta Biomater., 4 (2008) 1465-1471. https://doi.org/10.1016/j.actbio.2008.03.004.

***Declaration of Interest Statement**

Declaration of interests

☒ The authors declare that they have no known competing financial interests or personal relationships that could have appeared to influence the work reported in this paper.

☐The authors declare the following financial interests/personal relationships which may be considered as potential competing interests:

Figure 1

Click here to download high resolution image

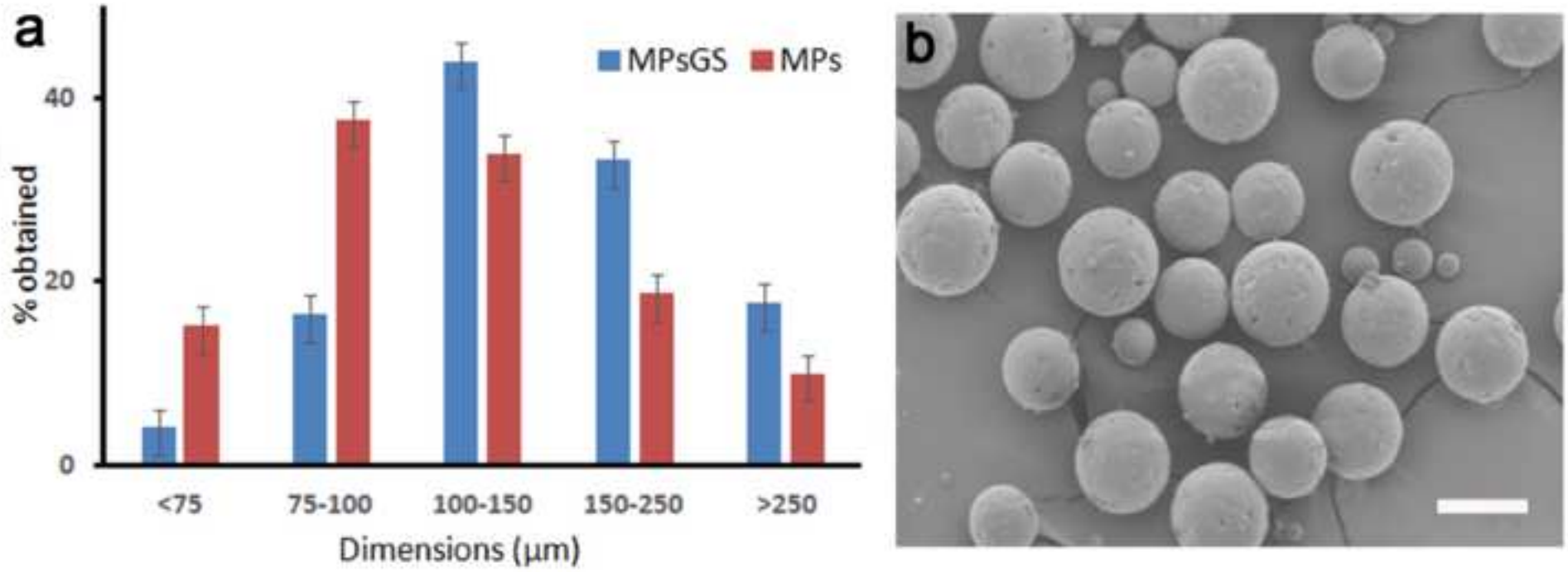

Figure 2

Click here to download high resolution image

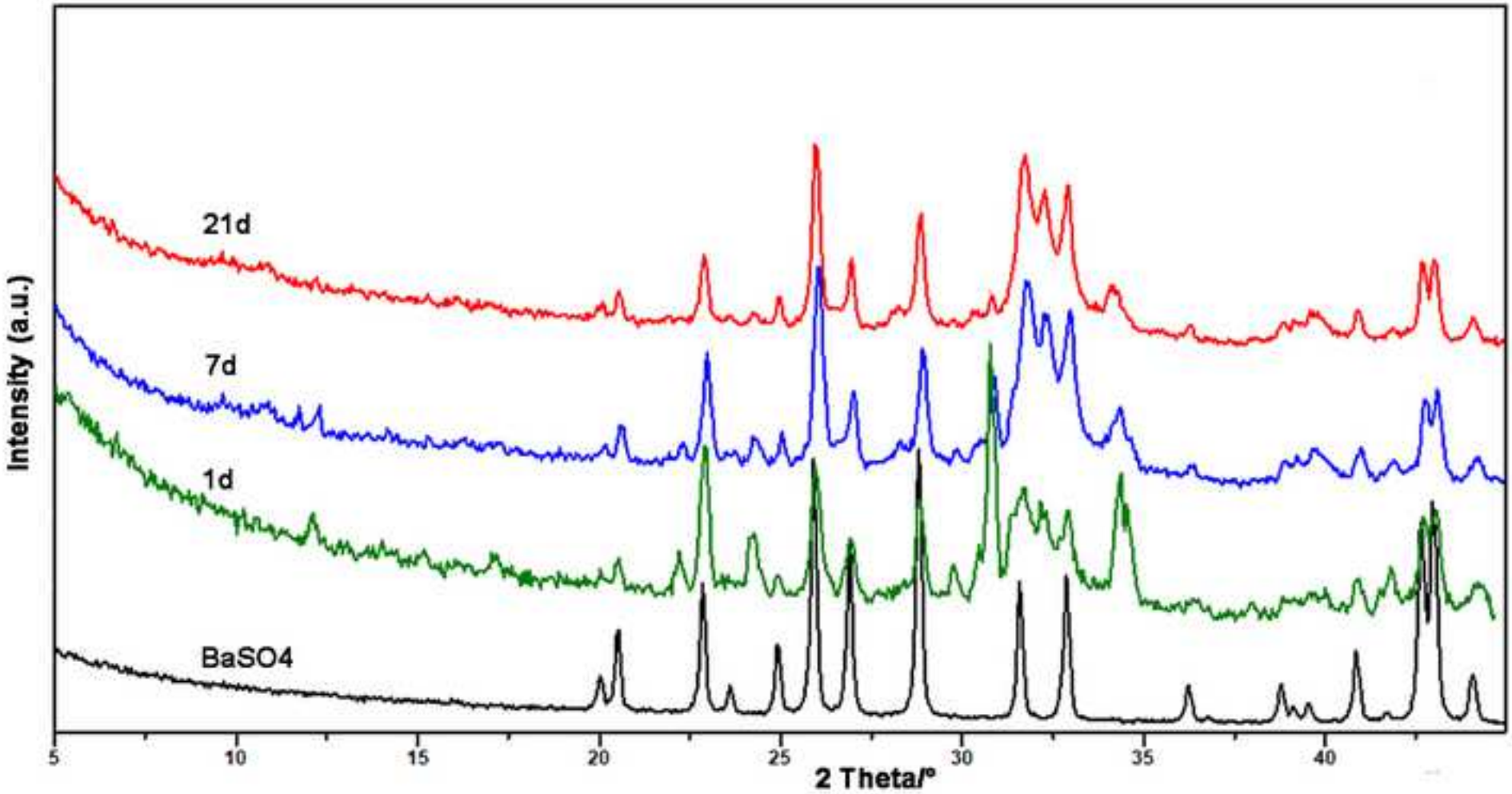

Figure 3

Click here to download high resolution image

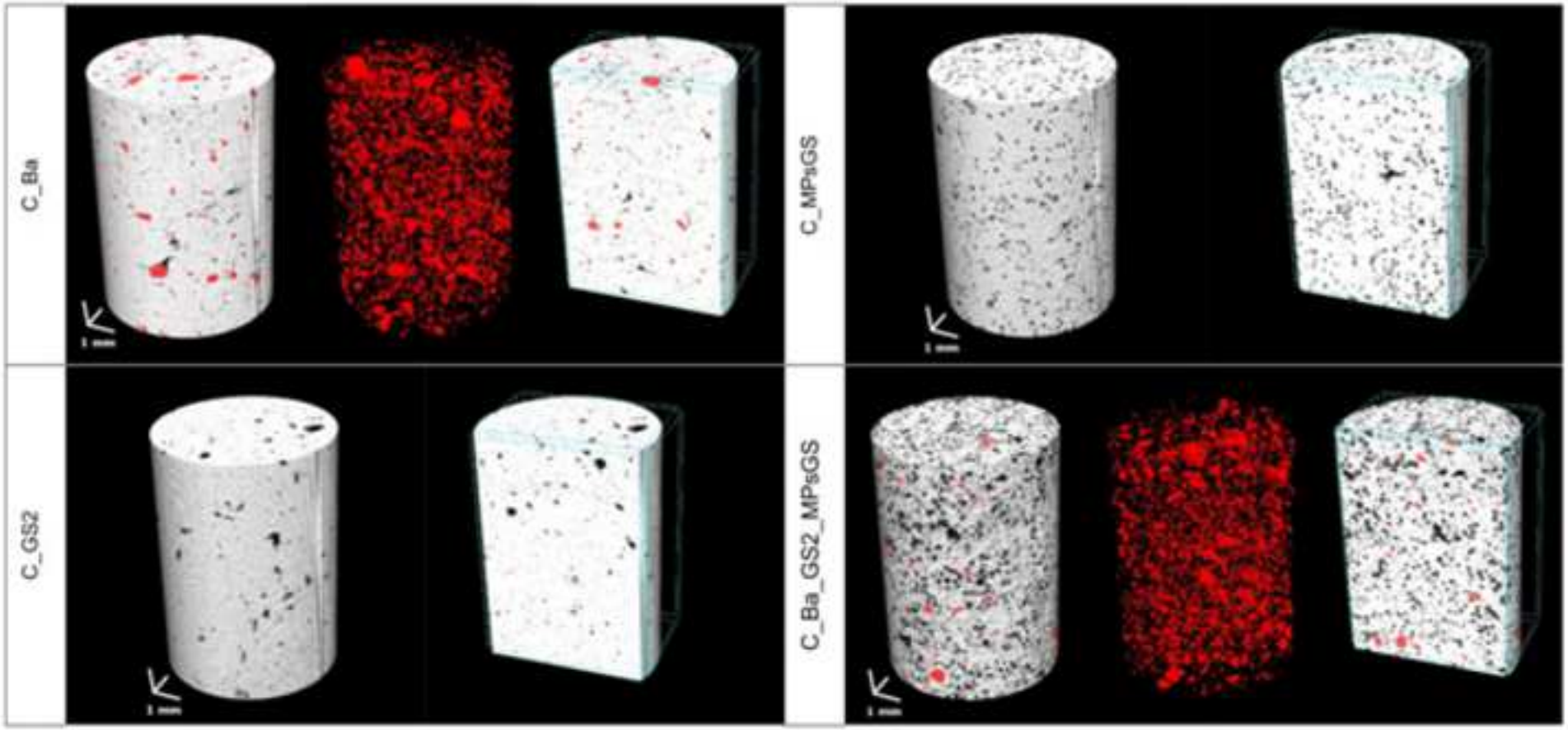

Figure 4

Click here to download high resolution image

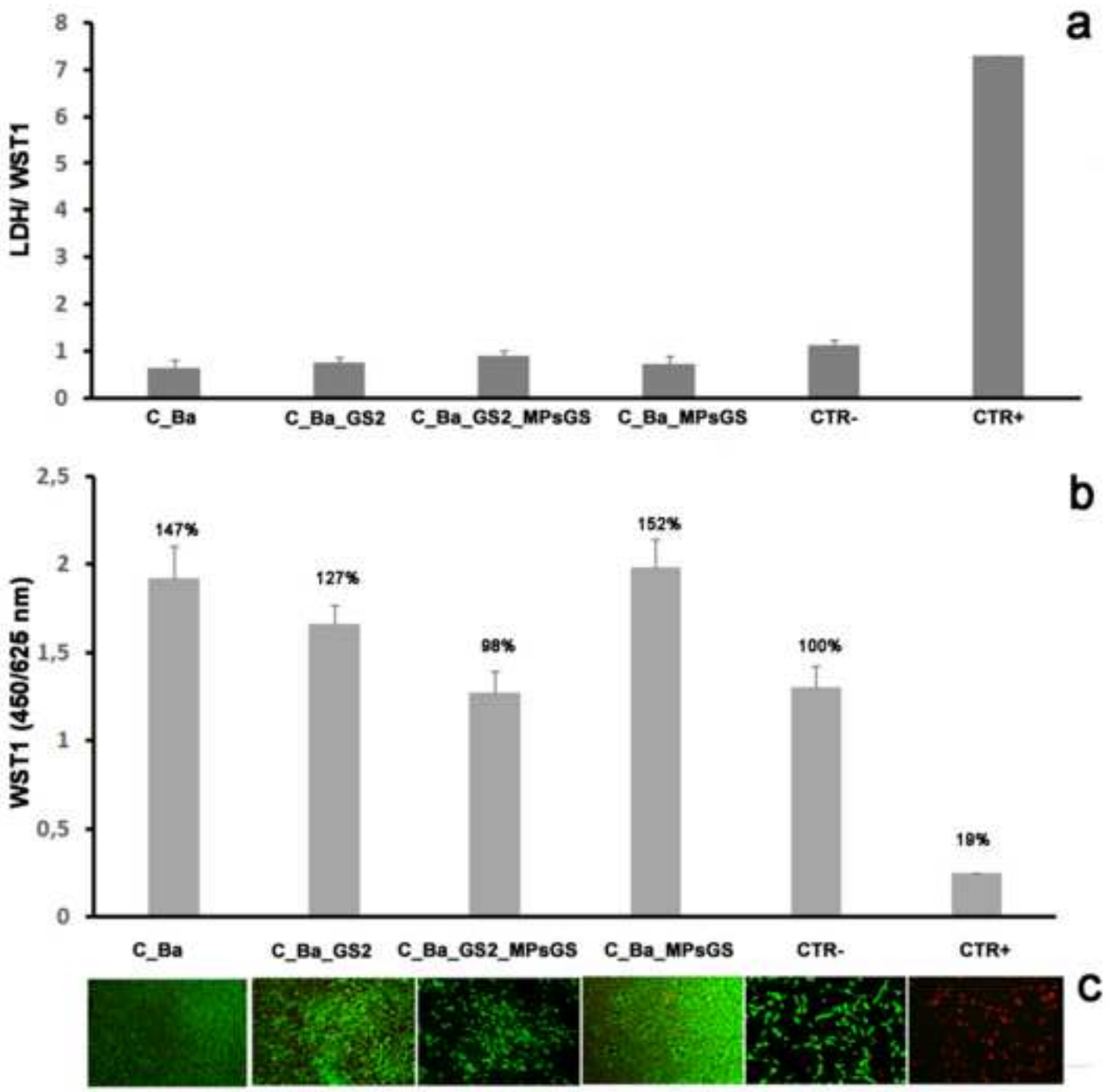

Figure 5

Click here to download high resolution image

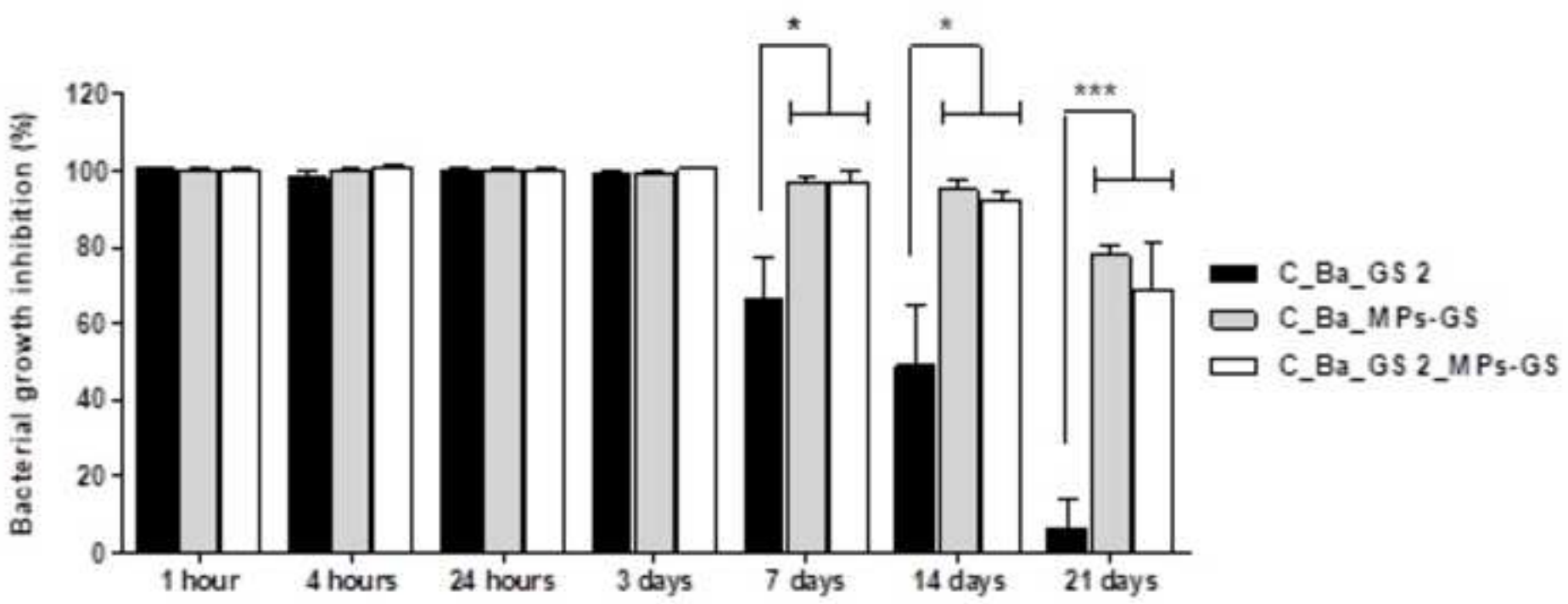

Figure 6

Click here to download high resolution image

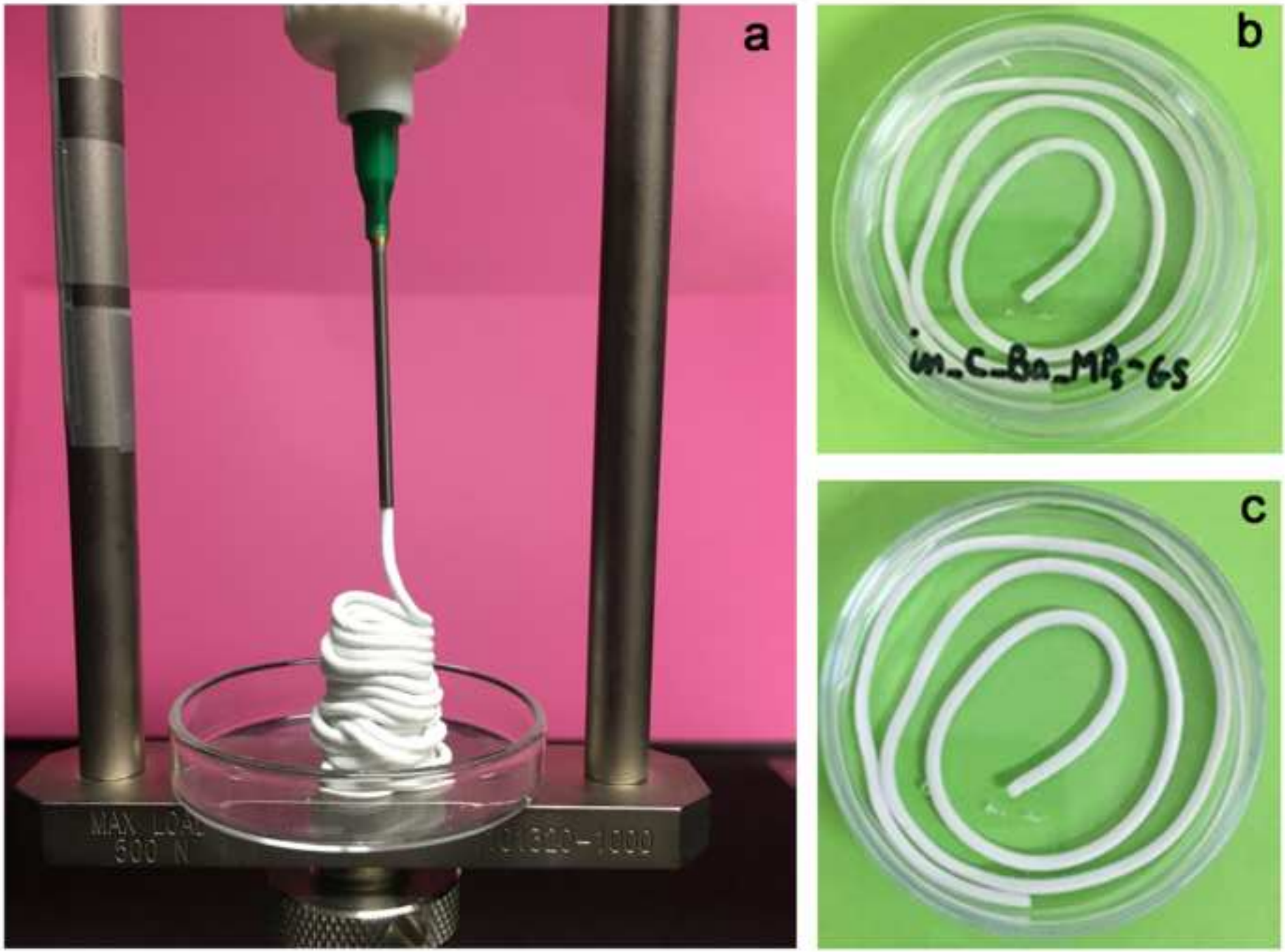

Figure 7

Click here to download high resolution image

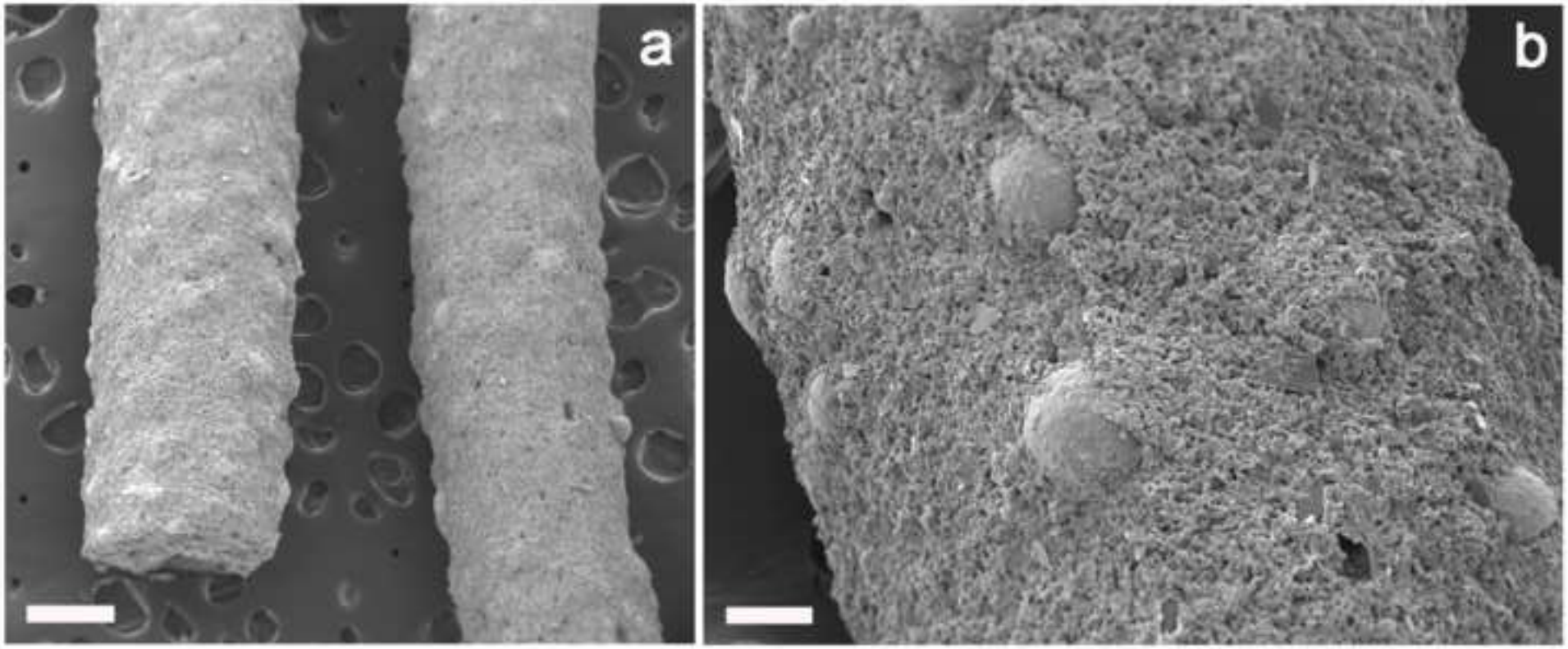

Figure 8

Click here to download high resolution image

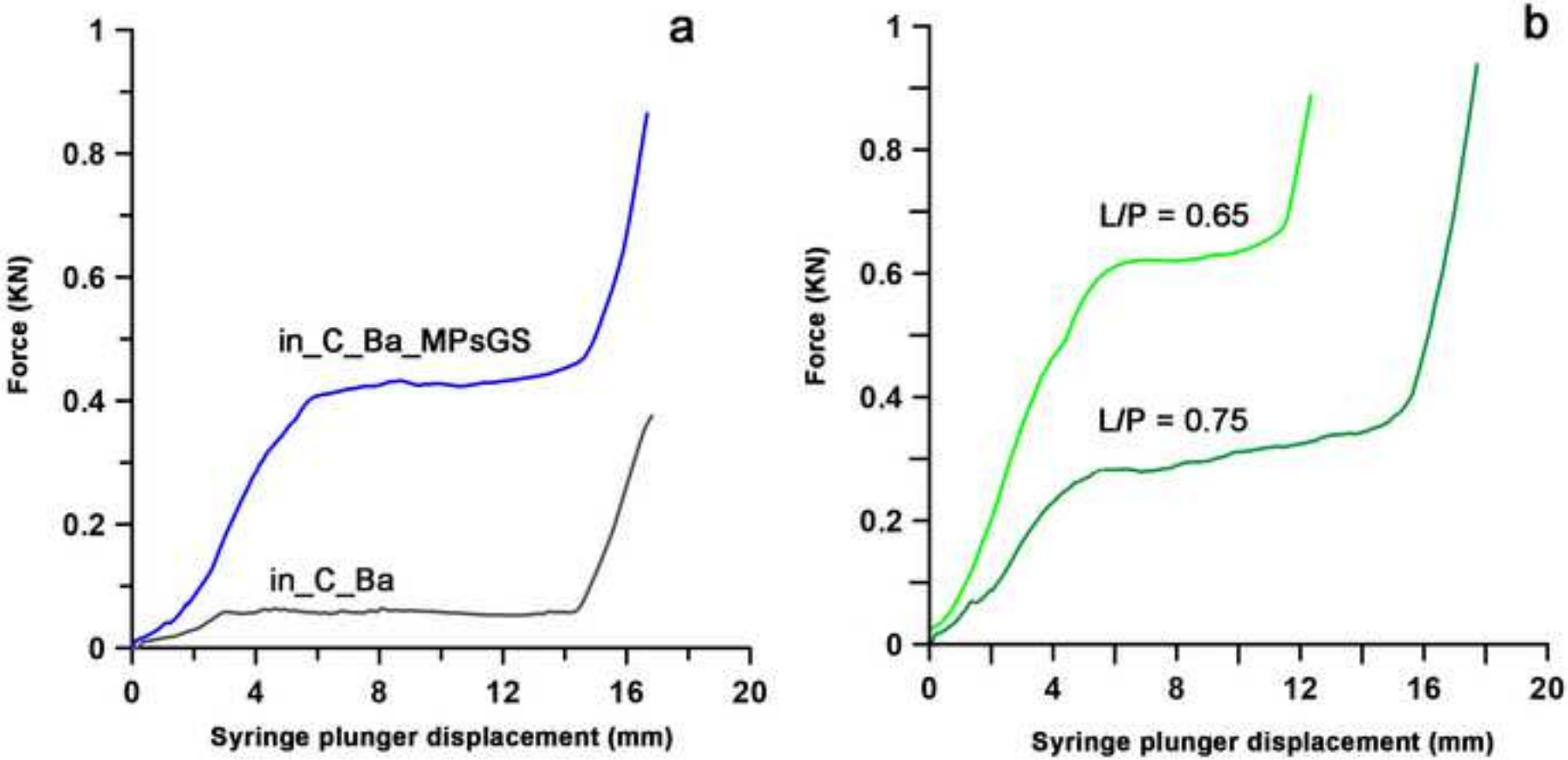

Graphical abstract

Click here to download high resolution image

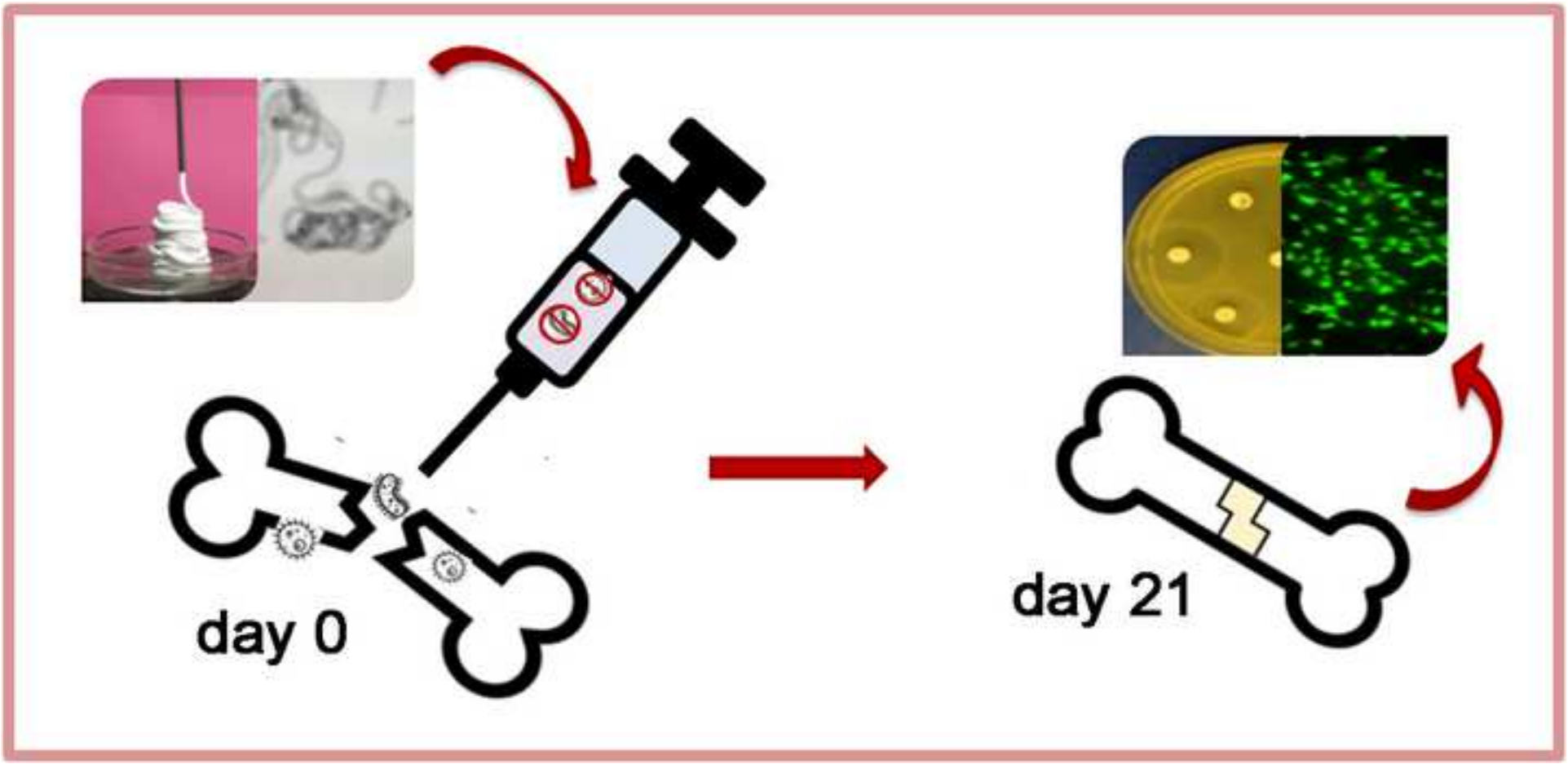

Captions

Figure 1 Particles size distribution of MPs and MPsGS (a) and SEM images of MPsGS (b). Bar = 100 μm.

Figure 2 X-Ray powder diffraction patterns recorded on C_Ba cements after different times of soaking, compared to BaSO4 pattern. The arrow indicates the most intense reflection of α-TCP.

Figure 3 3D models of representative samples analyzed by micro-CT. In every box the whole sample inside the VOI is shown on the left, the agglomerates of $BaSO_4$ are shown, where present, in the center colored in red, and the sample 3D model cut virtually along.

Figure 4 Cytotoxicity evaluation of MG63 osteoblast-like cell line after 72 hours of culture with biomaterials: (a) LDH, (b) viability by WST1 test, (c) Live & Dead staining (10x).

Figure 5. Antibacterial activity of GS released from disk-shaped samples (C_Ba_GS2, C_Ba_MPsGS and C_Ba_GS2_MPsGS) after incubation in PB solution up to 21 days. Values are means with standard deviations of two independent experiments. (*$p < 0.05$; *** $p < 0.0005$).

Figure 6 a) in_C_Ba_MPsGS cement extruded from the syringe during the injectability test; evaluation of cement cohesion put immediately in PB solution and photographed (b) immediately after extrusion and (c) after 24h.

Figure 6 Scanning electron microscopy of a cement wire in_C_Ba_MPsGS collected immediately after extrusion. Bar: a) 50 micron, b) 100 micron.

Figure 8 Injectability curves of a) in_C_Ba and in_C_Ba_MPsGS and b) in_C_Ba_GS 2_MPsGS with two different liquid to powder ratio.

Supplementary informations

Click here to download e-component: SI.docx

Video Still

Click here to download Video Still: video 1.mp4